Geophysical Research Letters

RESEARCH LETTER
10.1029/2019GL082513

Coherent South American Monsoon Variability During the Last Millennium Revealed Through High-Resolution Proxy Records

J. L. P. S. Campos[1], F. W. Cruz[2], T. Ambrizzi[1], M. Deininger[3], M. Vuille[4], V. F. Novello[2], and N. M. Strikis[5]

[1]Department of Atmospheric Sciences, Instituto de Astronomia Geofisica e Ciências Atmosféricas, Universidade de São Paulo, São Paulo, Brazil, [2]Department of Sedimentary Geology, Instituto de Geociências, Universidade de São Paulo, São Paulo, Brazil, [3]Institute of Geosciences, Johannes Gutenberg University Mainz, Mainz, Germany, [4]Department of Atmospheric and Environmental Sciences, State University of New York at Albany, Albany, NY, USA, [5]Department of Geochemistry, Universidade Federal Fluminense, Rio de Janeiro, Brazil

Key Points:
- We use high-resolution $\delta^{18}O$ records to decompose the South American Monsoon into its main modes of variability during the last millennium
- The first mode shows an enhanced monsoon during the Little Ice Age and a weakening during the Medieval Climate Anomaly
- The second mode represents monsoon variability along the fringes of the monsoon area and indicates periods of widening/contractions of the monsoon axis

Supporting Information:
- Supporting Information S1

Correspondence to:
J. L. P. S. Campos,
jose.leandro.campos@usp.br

Citation:
Campos, J. L. P. S., Cruz, F. W., Ambrizzi, T., Deininger, M., Vuille, M., Novello, V. F., & Strikis, N. M. (2019). Coherent South American Monsoon variability during the last millennium revealed through high-resolution proxy records. *Geophysical Research Letters*, *46*, 8261–8270. https://doi.org/10.1029/2019GL082513

Received 25 FEB 2019
Accepted 28 JUN 2019
Accepted article online 3 JUL 2019
Published online 17 JUL 2019

Abstract The number of paleoprecipitation records from the South American Monsoon domain that cover the last millennium has increased substantially in past years. However, hitherto most studies focused only on regional aspects, thereby neglecting the role of large-scale monsoon variability and the mechanisms that link proxy locations in space and time. Here we decompose the South American Monsoon into its main modes of variability by applying a Monte Carlo principal component analysis to a compilation of 11 well-dated summer paleoprecipitation records from tropical South America. The first mode represents changes in precipitation over the core monsoon domain, while the second mode is characterized by high loadings along the fringes of the South American Monsoon over Southeastern South America and the northern monsoon limit. Composite analysis reveals an enhanced monsoon with a wider, rather than a southward displaced, South Atlantic Convergence Zone during the early Little Ice Age, in contrast to previous interpretations.

Plain Language Summary The South American Monsoon is responsible for more than 70% of the annual precipitation falling over tropical South America. Due to the lack of data prior to the middle of the twentieth century, the long-term variability of the monsoon is poorly understood. Yet there are concerns that increasing greenhouse gas concentrations may significantly modify monsoon behavior in the 21st century. To better understand how the monsoon responds to such perturbations, detailed knowledge of how it varied in the past is crucial. This will facilitate improvements to Earth System Models that are used to project future rainfall changes in the region. Here 11 paleoprecipitation records that span the last millennium are analyzed using statistical techniques that allow extracting the shared variability from all records. Our result highlight how the monsoon responded in space and time to large-scale perturbations of the climate system, associated with the Little Ice Age and the Medieval Climate Anomaly.

1. Introduction

The tropical and subtropical South American climate is characterized by a monsoon circulation in austral summer, where the low-level winds converge over the eastern portion of the Amazon basin, transporting moisture westward into the continent. Blocked by the Andes, the flow forms a quasi-parallel "wind corridor" known as the northwest-southeast oriented South American Low-Level Jet (SALLJ), which, supported by midlatitudes transient weather systems, transports moisture from low to middle latitudes (Garreaud et al., 2009; Marengo et al., 2012; Vuille et al., 2012; Zhou & Lau, 1998). Over the continental midlatitudes (Paraguay and northern Argentina) a baroclinic thermal Low forms near the surface, the Chaco Low, leading to a cyclonic circulation over the La Plata Basin. This thermal Low, together with the anticyclonic circulation of the South Atlantic Subtropical High, supports the SALLJ and the low-level (850 hPa) moisture convergence, favoring deep convection, characterizing the monsoon axis or the South Atlantic Convergence Zone (SACZ, Kodama, 1992), schematically represented in Figure 1. The baroclinic upper-level (300 hPa) counterparts to the Chaco Low and the subtropical High, the Bolivian High and an upper-level cyclonic vortex, known as the Northeast Trough (Chen et al., 1999; Lenters & Cook, 1999), form an upper-level ridge (upper-level divergence region), which defines the position and shape of the monsoon axis.

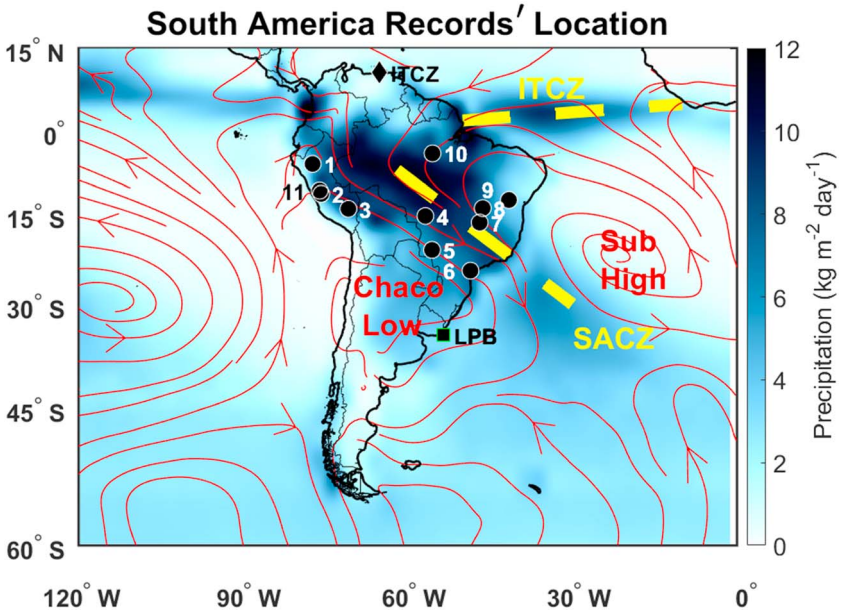

Figure 1. The 850-hPa monsoon circulation and location of isotopic proxy records used in the present study. The dots in the figure represent the record locations and the shading represents the mean summer (December–February) precipitation climatology extracted from 30 years (1981–2010 CE) of Global Precipitation Climatology Project data. The red streamlines represent the austral summer (December–February) 850-hPa circulation. The Intertropical Convergence Zone (ITCZ) and South Atlantic Convergence Zone (SACZ) are represented by the yellow dotted lines. The location of two nonisotopic marine records of continental runoff from the La Plata Basin (LPB) and the Cariaco Basin (ITCZ) are represented by a square and diamond, respectively.

The South American Monsoon is fueled by water vapor originating over the tropical Atlantic Ocean. The lack of a substantial temperature gradient during moisture transport across the tropical continent facilitates the application and interpretation of stable water isotopologues such as $\delta^{18}O$, suitable for paleoprecipitation studies within a Rayleigh distillation framework (Hurley et al., 2016; Novello et al., 2018; Vuille et al., 2012; Vuille & Werner, 2005). During the last decade the number of available $\delta^{18}O$ records has increased significantly, resulting in a network of geographically well-dispersed records across the South American Monsoon area. Recent efforts to integrate multiple South American paleoprecipitation records have focused on the comparison of $\delta^{18}O$ time series across eastern Brazil, revealing a precipitation dipole across the SACZ region during last millennium (Deininger et al., 2019; Novello et al., 2018). In general, $\delta^{18}O$ records from speleothems, lake sediment calcite, and ice cores in the tropical Andes (Apaéstegui et al., 2014; Bird et al., 2011; Kanner et al., 2013; Thompson et al., 2013) and south central Brazil (Novello et al., 2016; Novello et al., 2018) contain a common signal that can be traced to their joint history of upstream rainout over the Amazon basin (Hurley et al., 2016; Vuille et al., 2012; Vuille & Werner, 2005). At the same time multiple local calibration studies have also documented that these isotopic records are significantly correlated with local precipitation at the cave sites (e.g., Moquet et al., 2016; Novello et al., 2016). Hence, we interpret changes in the $\delta^{18}O$ time series as variations in monsoon intensity and also local hydrologic conditions at the respective locations where the proxies were sampled. These records all suggest that an anomalously drier climate prevailed during the Medieval Climate Anomaly (MCA, CE 950–1250; Intergovernmental Panel on Climate Change (IPCC), 2009) and anomalously wetter conditions dominated the region during the Little Ice Age (LIA, CE 1450–1850; IPCC, 2009). In Northeastern Brazil (NEB) on the other hand, speleothems (Novello et al., 2012; Novello et al., 2018) indicate no changes in precipitation amounts during the MCA and a drier LIA but a wetter transitional period (TRANS, CE 1250–1450; IPCC, 2009). However, a better characterization of the spatial and temporal coherence of monsoon variability as recorded in these discrete records is clearly needed, as is a more thorough analysis of the forcing mechanisms that are consistent with the observed monsoon variability in space and time. Here we provide an analysis of the spatiotemporal variability of the South American Monsoon, based on a quantitative decomposition of the existing records into

Table 1
Proxy Records Analyzed

Records	ID	Isotope	Latitude	Longitude	Mean sampling	Reference
PAL03+PAL04	1	$\delta^{18}O_{cal}$	5.92°S	77.35°W	5.0 years	Apaéstegui et al. (2014)
HUA	2	$\delta^{18}O_{cal}$	11.27°S	*75.79°W*	5.0 years	Kanner et al. (2013)
QUELC	3	$\delta^{18}O_{ice}$	13.93°S	*70.83°W*	1.0 year	Thompson et al. (2013)
ALH+CUR4	4	$\delta^{18}O_{cal}$	15.20°S	56.80°W	0.6 year	Novello et al. (2016)
JAR1+JAR4	5	$\delta^{18}O_{cal}$	21.08°S	55.58°W	2.5 years	Novello et al. (2018)
CRT	6	$\delta^{18}O_{cal}$	24.58°S	48.58°W	2.7 years	Vuille et al. (2012)
TMO	7	$\delta^{18}O_{cal}$	16.00°S	47.00°W	3.6 years	Wortham et al. (2017)
SBE3+SMT5	8	$\delta^{18}O_{cal}$	13.81°S	46.35°W	1.2 years	Novello et al. (2018)
DV2+TR5+LD12	9	$\delta^{18}O_{cal}$	12.36°S	41.57°W	4.0 years	Novello et al. (2012)
PAR01+PAR03	10	$\delta^{18}O_{cal}$	4°4′S	55.45°W	7 years	Wang et al. (2017)
PUM	11	$\delta^{18}O_{cal}$	10.07°S	76.06°W	1 year	Bird et al. (2011)

Note. Time series of the individual proxy records are provided in the supporting information. The location of the records is illustrated in Figure 1.

two main modes of variability that explain most of the total variance observed during the past 1,000 years. The analysis is based on a compilation of 11 well-dated paleoclimatic records from the South American Monsoon domain, employing the Monte Carlo principal component analysis (PCA) method (Anchukaitis & Tierney, 2013; Deininger et al., 2017).

2. Materials and Methods

In Table 1 and Figure 1 the locations of the eleven $\delta^{18}O$ isotopic time series are presented (the records' time series are presented in supporting information Figure S1). Almost all records cover the period from CE 600 to CE 1970 (supporting information Table S1). The only exceptions are record #1 (PAL03 + PAL04) and #4 (ALH + CUR4), which span up to CE 1928 and CE 1964, respectively. In order to extend these records to 1970, the alternate least squares algorithm was applied during the PCA. Some time series were obtained by merging two or three records as indicated in Table 1. In order to "merge" these records, each isotopic time series was annually synchronized using a cubic spline during the overlap period. Each record was then normalized to unitary variance (z-scores) and averaged into one time series. Finally, the time series was reconstructed using the inversion of the normalization of the longer time series (using standard deviation and the mean of the longer time series).

In order to account for the dating uncertainty of each proxy record, a linear age-depth model was constructed for each record accounting for $\pm 1\sigma$ in the dating uncertainty. Through a set of 1,000 Monte Carlo simulations, where a random age within the $\pm 1\sigma$ age interval was chosen each time, 1,000 age models for each isotopic record were produced. The corresponding proxy time series were obtained through interpolation between the ages using the linear age-depth model (in the supporting information a figure of the age-depth model is provided). Finally, each proxy time series was synchronized and sampled to an annual resolution before undergoing a low-pass filtering at the band of 30^{-1} year^{-1}, in order to account for differences in the records' original temporal resolution (for details see the supporting information).

Eleven time series, one for each record, were randomly chosen from the ensemble produced by the Monte Carlo simulations and subjected to a PCA, resulting in 11 spatial patterns (loading coefficients) and 11 principal components (PCs) or scores (time series representing the standing oscillation of the spatial patterns). This procedure was repeated 1,000 times, the number of Monte Carlo simulations (see Anchukaitis & Tierney, 2013; Deininger et al., 2017). More details on the methods are supplied in the supporting information.

3. Results

3.1. Leading Modes of Monsoon Variability

The first and second Monte Carlo PCs were retained in this study, representing 30 ± 2% and 13 ± 1% of the total $\delta^{18}O$ variability (see supporting information Figure S2), respectively. To compare the isotope-derived main modes of monsoon variability with present-day low-frequency precipitation patterns (Figure 2, see

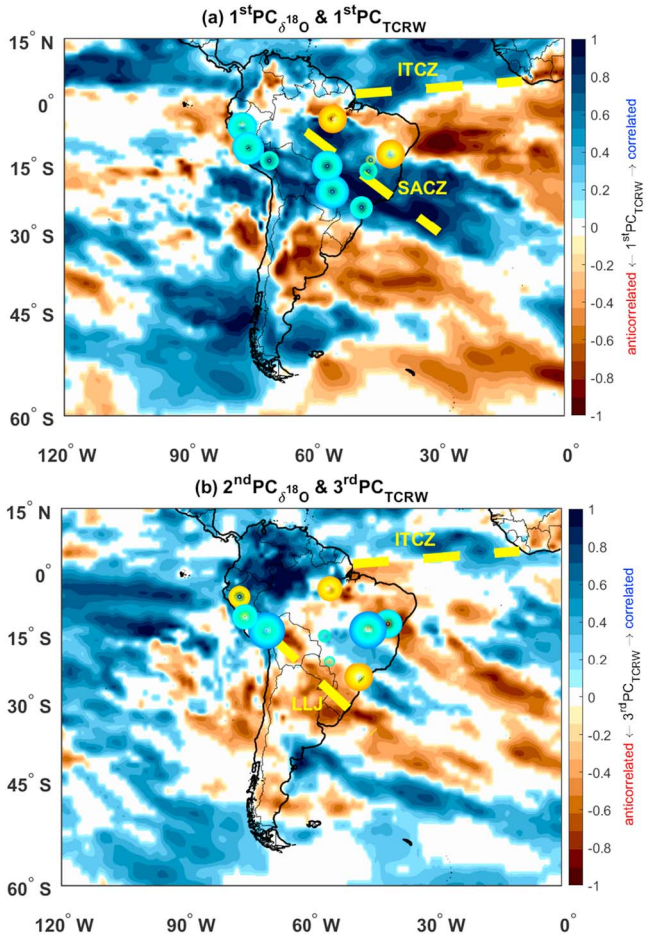

Figure 2. Comparison between proxy- and reanalysis-derived main monsoon modes. (a) First $PC_{\delta^{18}O}$ and (b) second $PC_{\delta^{18}O}$. The dots in the figures represent the proxy records and the shading indicates the first and third principal component computed with 110 years (CE 1901–2010) of CERA-20C Total Column Rain Water (TCRW) reanalysis data. The size of the dots corresponds to the loading coefficient magnitude, the blue and brown colors represent positive and negative loadings of the $\delta^{18}O$ time series, respectively. The larger the dot, the stronger its correlation with the respective proxy-derived principal component. The dashed yellow lines represent significant monsoon subcomponents, the Intertropical Convergence Zone (ITCZ) and the South Atlantic Convergence Zone (SACZ). LLJ = Low-Level Jet.

supporting information Table S1 and Figure S3 for details), a PCA of 110 years (CE 1901–2010) low-pass-filtered (>30 years) Total Column Rain Water (PC_{TCRW}) CERA-20C reanalysis data (twentieth century Coupled European Reanalysis; Laloyaux et al., 2018) was evaluated. The first and third PC_{TCRW} spatial patterns (loadings or empirical orthogonal functions), explaining 42% and 13% of data variability, were associated (see supporting information Figure S7), with the first and second $PC_{\delta^{18}O}$, respectively.

The spatial patterns of the first $PC_{\delta^{18}O}$ and the first PC_{TCRW} show similar spatial characteristics for most of the records analyzed (Figure 2a). The leading mode derived from the $\delta^{18}O$ time series represents a dipole between the core monsoon region (blue colored dots, positive correlation) and the north and northeast region of Brazil (brown colored dots). The latter is represented by the speleothems #9-DV2, #10-PAR, and #8-SBE. This dipole is consistent with the seesaw between the northeastern and southeastern portions of the South American Monsoon region suggested by Novello et al. (2018) and also seen in present-day precipitation data (e.g., Sulca et al., 2016). Novello et al. (2012) also showed that precipitation over the eastern Amazon varies in phase with precipitation over NEB and out of phase with isotopic proxies from the central Andes (#2-HUA and #3-QLC). A linear correlation in space between the first $PC_{\delta^{18}O}$ and the low-frequency TCRW data during the Current Warm Period (CE 1902–1970) results in very similar patterns (supporting information Figure S6).

The second $PC_{\delta^{18}O}$ shows a configuration, where proxy records in the southern tropical Andes (#2-HUA and #3-QUELC) and eastern Brazil (#8-SBE and #9-DV2) are positively correlated with the second $PC_{\delta^{18}O}$, while records from the more equatorial tropical Andes (#1-PAL and #11-PUM), the central Amazon (#10-PAR) and southeastern Brazil (#6-CRT) vary out of phase (Figure 2b). The remaining records (notably in the south central Amazon) have small loading coefficients, indicating that they are not closely correlated with this mode. The third PC_{TCRW} presents a similar pattern as seen in the proxy data (Figure 2b).

3.2. Time Series Analyses

The temporal variability of the two leading monsoon modes described above (Figure 2) is represented by their respective PCs or time expansion coefficients (Figures 3a and 3b). Negative values of these PCs indicate periods of positive precipitation anomalies at locations where the correlation between the PC and the $\delta^{18}O$ time series is positive (Figure 2). A change point detection test, based on the sample mean (*Lavielle,* 2005), was performed over the first and second $PC_{\delta^{18}O}$. Five change points were detected for first $PC_{\delta^{18}O}$ (Figure 3a), dividing the time series into four distinct climate periods or regimes. These periods can be assigned to the MCA (CE 724–1160), a transitional period (TRANS, CE 1160–1489), the LIA (CE 1489–1878), and the Current Warm Period. The same test was applied to the second $PC_{\delta^{18}O}$ (Figure 3b) as well as to the marine records of continental runoff from the La Plata basin and the Cariaco basin (Haug et al., 2001; Figure 3d), respectively.

The dates of onset and demise of the identified climatic periods in this study differ from dates reported in the IPCC (2009), but these are based on Northern Hemisphere last millennium temperature, which may explain this discrepancy. Previous studies in South America (Apaéstegui et al., 2014; Novello et al., 2012) used subjective criteria based on wavelet analysis, to determine the onset and the demise dates for these climate periods and came to different conclusions as well, particularly for the LIA period. This highlights the

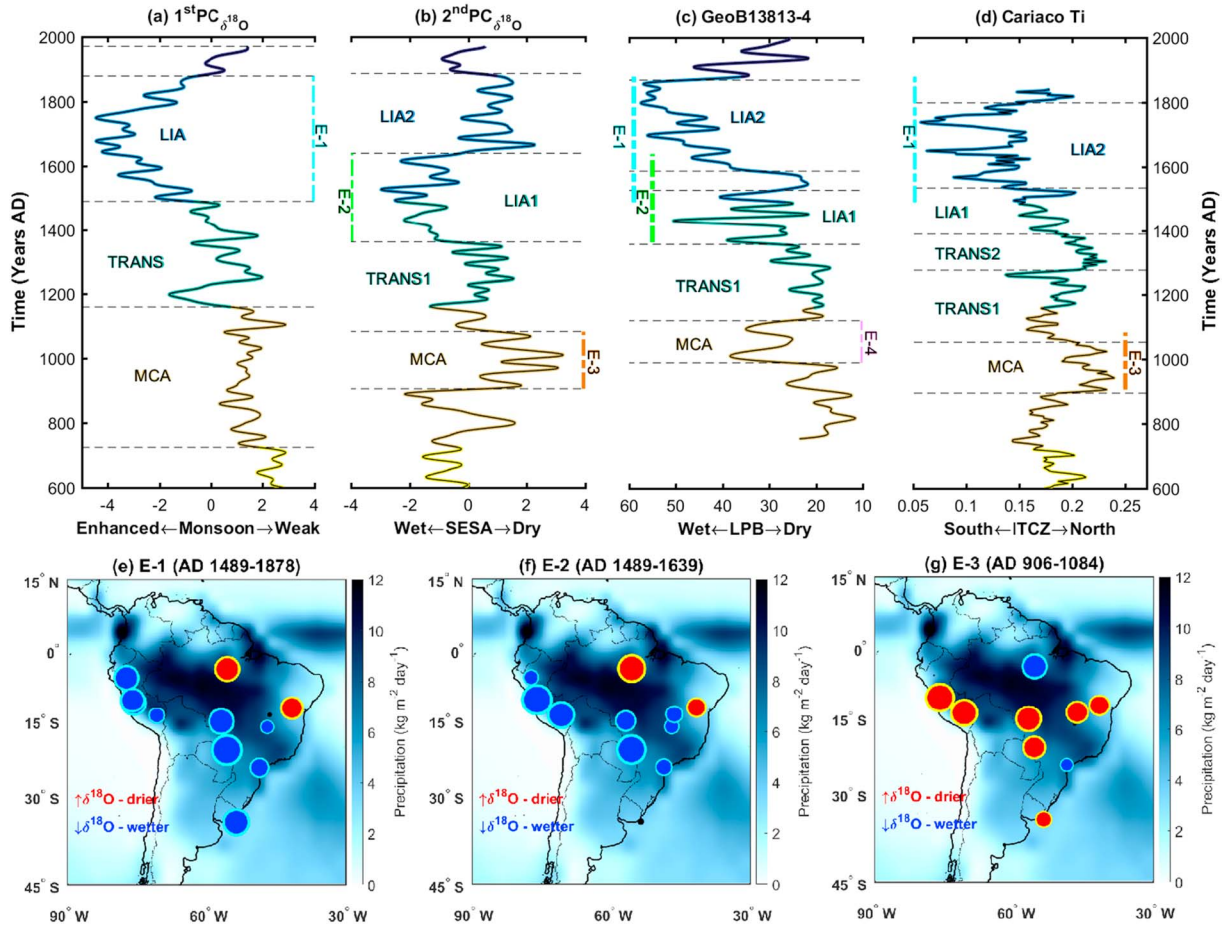

Figure 3. Precipitation variability over South America during the Last Millennium. (a) First $PC_{\delta^{18}O}$ mode, (b) second $PC_{\delta^{18}O}$ mode, (c) fresh water diatomaceous percentage on the La Plata river estuary (Perez et al., 2016), and (d) Cariaco Basin sediment Titanium ratio (Haug et al., 2001). The colors represent the different climate regimes found through a change-point detection test based on the mean, evaluated on the first $PC_{\delta^{18}O}$. The dotted lines represent change points detected with the respective time series. (e) Event 1 E-1, (f) Event 2 E-2, and (g) Event 3 E-3. The dots represent normalized $\delta^{18}O$ anomalies with respect to the period CE 600–1970, with red dots indicating positive $\delta^{18}O$ anomalies and blue dots negative $\delta^{18}O$ anomalies; the blue shading represents the mean precipitation climatology for the period CE 1980–2010. The marine sediment record GeoB13813-4 was also included in the maps.

spatiotemporal variability in the timing of these climatic periods across tropical South America (further details can be found in supporting information Table S3).

4. Discussion

Given the strong similarity between the proxy- and the TCRW-derived leading modes, PC1 is interpreted as the monsoon variability mode, representing the spatiotemporal variability of convective activity over the core monsoon domain. This is because strong convective activity over the core monsoon region provokes an intensification of the east-west dipole, in turn reducing precipitation amounts in NEB (Cruz et al., 2009; Sulca et al., 2016), while precipitation amounts increase in the other monsoon regions. Furthermore, Novello et al. (2012) demonstrated that under such conditions, meridional Intertropical Convergence Zone (ITCZ) shifts become less influential in determining precipitation amounts in NEB. The variability of the first $PC_{\delta^{18}O}$ during the last millennium (Figure 3a) shows strong excursions toward negative values during the LIA, indicating enhanced precipitation over the western, south central, and southeastern portions of tropical South America, balanced by reduced precipitation in northeastern South America, consistent with results from previous studies (see references in Table 1 and Deininger et al., 2019). During the MCA, positive values indicate reduced precipitation, with even stronger positive values in the period preceding the onset of the MCA.

The second PC shows a pattern that is reminiscent of monsoon contraction and expansion with antiphased precipitation behavior along the northern and southern edges of the monsoon belt, when compared to its core region. We therefore interpret this PC as representing periods of monsoon widening or contraction, but we also caution that this mode is defined by few records along the fringes of the monsoon belt and that additional records will be required to develop a more robust picture of this mode of variability. The second $PC_{\delta^{18}O}$ undergoes five regime shifts (Figure 3b). The MCA and the second half of the LIA (LIA2) are characterized by positive values, indicating dry anomalies over the northern monsoon border and over southeastern South America (regions with positive loadings in Figure 2b), whereas the early part of the LIA (LIA1) was anomalously wet in these regions.

The comparison with a precipitation reconstruction for the La Plata Basin from GeoB13813-4 (Perez et al., 2016; Figure 3c) shows the same excursion toward wet anomalies (higher freshwater diatom percentage) during the LIA period as seen in the first $PC_{\delta^{18}O}$, indicative of a stronger monsoon. The La Plata drainage basin is a region that can receive high precipitation amounts during both strong and weak monsoon regimes. High runoff of the La Plata River can be caused by positive precipitation anomalies over the northern and southern portions of the basin, that are influenced by convective activity over the southwestern Amazon basin or midlatitude transients and extreme SALLJ events during weak monsoon episodes, respectively (Salio et al., 2007). For example, a "wet" excursion appears over the La Plata basin during the MCA, (labeled as event E-4 in Figure 3c), despite dry anomalies over the northern portion of the La Plata basin, likely indicating a higher frequency of transient extratropical weather systems (e.g., cyclones, cold fronts, and mesoscale convective systems).

The monsoon mode represents the dominant signal in the $\delta^{18}O$ data, indicating that the LIA was the wettest period over South America during the last millennium (event E-1 in Figure 3a). The LIA signal is present in all time series, albeit with varying timing of onset and demise. The second $PC_{\delta^{18}O}$, in particular shows an early onset and demise of the LIA. In the GeoB13813-4 sediment record the onset is delayed, but the demise is synchronous with the first $PC_{\delta^{18}O}$. The Cariaco %Ti record (Haug et al., 2001; Figure 3d) is highlighting the displacement of the ITCZ, and is intimately tied to the South America Summer Monsoon (SASM) intensification (first $PC_{\delta^{18}O}$,), consistent with the ITCZ-SASM relationship discussed in Vuille et al. (2012), although in the Cariaco %Ti record the LIA period ends a bit earlier (Figure 3d).

The composite analysis for the LIA (E-1, Figure 3e), CE 1489–1878, reveals wet anomalies over the core monsoon domain, including the southern Amazon, the tropical Andes and the SACZ, whereas stronger dry anomalies ($>+1\sigma$, see supporting information Table S4) prevail over northern and NEB (represented by records #9-DV2 and #10-PAR). The La Plata River Basin record (Figure 3c) indicates enhanced fresh water input, consistent with its role as a proxy integrating the hydrologic response over a large watershed covering parts of the southern monsoon domain. Overall, our result suggests that during the LIA, the South American Monsoon was enhanced, consistent with previous studies (Apaéstegui et al., 2014; Bird et al., 2011; Deininger et al., 2019; Kanner et al., 2013; Vuille et al., 2012).

The wettest period of the second monsoon mode (Figure 3b) occurred during the LIA1 period (event E-2). This period overlaps with the wettest period in the first $PC_{\delta^{18}O}$ (event E1, CE 1489–1639), a time when anomalously wet conditions dominate throughout the main monsoon domain (see composite in Figure 3 f). The only regions where conditions remained near average at this time are found over the La Plata basin, while northern and NEB experienced dry conditions. The high-elevation Andean records Pumacocha (#1-PUM) and Quelccaya (#3-QLC) along the southwestern edge of the monsoon domain indicate wetter conditions at this time than during E-1, suggesting an enhancement of moisture transport from the western Amazon basin to the Andes (Garreaud et al., 2003; Hurley et al., 2015). The records #7-TMO and #8-SBE, located to the south of the NEB region, also present slightly wetter conditions than during the event E-1, indicating a northeastward expansion of the monsoon axis.

The MCA period is a more pronounced dry event in the second $PC_{\delta^{18}O}$ (event E-3, Figure 3b) than in the first $PC_{\delta^{18}O}$ but expressed as a wet event in the GeoB13813-4 record (event E4, Figure 3c). During this period drier conditions persist at almost all other locations, except Paraiso Cave, located in eastern Amazonia (#10-PAR), and Cristal Cave, located in southeastern Brazil (#6-CRT1). During this period, positive %Ti anomalies are recorded at the Cariaco Basin (Figure 3d), consistent with the notion of a northward

displaced Atlantic ITCZ, evidencing again the relationship between monsoon intensity and the latitudinal position of the ITCZ (Vuille et al., 2012; see also supporting information Figure S8). The wet pulse observed at that time in the GeoB13813-4 data (event E4) and in Cristal Cave suggests higher activity of extratropical transient systems along the southern monsoon margin during this period.

Some authors, such as Novello et al. (2018) and Bernal et al. (2016), analyzed $\delta^{18}O$ and Sr/Ca composite means during the MCA and LIA but considered only the latitudinal position of the records, which led them to suggest that a southward displacement of the SACZ or the monsoon axis took place during the LIA. However, the analysis of all existing isotopic records indicating South American Monsoon variability suggests an intensified SACZ associated with an enhanced monsoon preserved its shape throughout much of this period (Figure 3f), except during its onset (E2, Figure 3b). The enhancement of the monsoon during the LIA is directly connected to the southward shift of the ITCZ, which leads to an enhanced moisture influx from the tropical Atlantic toward tropical South America (Vuille et al., 2012), thereby enhancing the moisture convergence and convection over the monsoon region.

The subtropical South Atlantic represents another important monsoon forcing, forming a sea surface temperature (SST) dipole between the tropical and subtropical South Atlantic, coupled to the overlying sea level pressure of the Subtropical High (Chaves & Nobre, 2004; Jorgetti et al., 2014; Utida et al., 2019). When in its positive phase, the colder SSTs to the south and warmer SSTs equatorward enhance the anticyclonic circulation associated with the Subtropical High and hence the inland moisture influx, thereby favoring the formation of the SACZ. In its negative phase, on the other hand, the Subtropical High is suppressed, favoring the intrusion of transient extratropical systems, such as extratropical cyclones and frontal systems, which lead to the characteristic northwest-southeastward orientation of the monsoon circulation over SESA (Southeast South America). Unfortunately, the lack of high-resolution marine records from the last millennium in the South Atlantic precludes a more thorough assessment of the role of the South Atlantic in forcing the South American Monsoon during the last millennium (see Utida et al., 2019).

In the current climate, when the monsoon axis is active, positive precipitation anomalies dominate over the SACZ domain, while precipitation is reduced over NEB and SESA (Silva & Berbery, 2006). This occurs as the enhanced convection over the SACZ is balanced by increased subsidence over the surrounding regions and by the action of midlatitude Rossby wave trains propagating northeastward from the tropical Pacific Ocean in an arch-like trajectory (Carvalho et al., 2004; Ma et al., 2011; Muza et al., 2009). Such a pattern is observed during the LIA in event E2, where the NEB records (#10-DV2 and #11-PAR) present signals that are opposite to the core monsoon records, while the La Plata record shows no significant anomalies (Figure 3f). However during the latter period of the LIA (E1) and the MCA (E3), (Figures 3f and 3g), this pattern is not apparent, suggesting possible changes or displacements in the monsoon circulation and Rossby waveguides (Hoskins & Ambrizzi, 1993) during these times.

Wavelet and spectral analyses (see the supporting information) were performed on the first and second $PC_{\delta^{18}O}$ revealing significant periodicities at 256, 128, 70, and 32 years. Previous studies, such as Novello et al. (2012), Apaéstegui et al. (2014), Bernal et al. (2016), and Perez et al. (2016), have argued that the longer cycle periodicities (128 and 256 years) can be attributed to solar variability and multidecadal internal variability such as the AMO (Atlantic Multidecadal Oscillation). Recent studies by Jones and Carvalho (2018) show a possible influence of the AMO on South American hydroclimate over the last 100 years. The AMO, in its positive phase, shifts the ITCZ northward following the warming of the subtropical North Atlantic, thereby increasing the cross-equatorial flow over northwestern South America and subsidence over northern Amazonia. This subsidence results in an enhancement of the meridional flow and more humid conditions over subtropical South America. Multiple studies have documented a past role of the AMO in modulating the South American Monsoon on multidecadal time scales (Chiessi et al., 2009; Parsons et al., 2014). Hence, the AMO may have affected the behavior of the monsoon, especially during the MCA and LIA1 period, when the GeoB13013-4 (Figure 3c) sediment record indicates exceptionally wet excursions during event E4 and at the beginning of event E2.

5. Conclusions

The Monte Carlo PCA of 11 well-dated paleoprecipitation proxies from across tropical South America reveals two main modes of monsoon variability. The first mode is characterized by a southwest-northeast

oriented dipole, representing monsoon strength over the core monsoon region, extending from the tropical Andes to eastern Brazil, with antiphased monsoon strength in NEB. This mode is associated with an enhanced monsoon during the LIA and a weakened monsoon during the MCA period. The second mode presents action centers toward the edges of the monsoon domain and therefore serves to characterize changes in the extent of the monsoon. This mode indicates drier conditions over southeastern South America during the early part of the LIA and wetter conditions during the late phase of the LIA.

Composite analyses and comparisons between the MC-PCA and the marine sediment record GeoB13813-4 (Perez et al., 2016), representing the integrated precipitation over the La Plata Basin drainage area, suggest a widening of the monsoon domain during the early LIA period (CE 1489 to CE 1639). This result yields an alternative explanation to the spatiotemporal precipitation variability seen in the various (individual) proxy records, when compared to earlier studies which suggested that the SACZ or the monsoon axis was displaced southward during all the LIA (Apaéstegui et al., 2018; Bernal et al., 2016; Deininger et al., 2019; Novello et al., 2018).

The South American Monsoon domain by now features a rich archive of spatially well distributed high-resolution paleoprecipitation records covering the last millennium. This data set can now be exploited to analyze the multidecadal evolution of monsoon precipitation and associated circulation systems such as the SACZ and the ITCZ. However, further efforts to recover additional paleoprecipitation records in under-sampled regions such as Amazonia, NEB, and the La Plata Basin are needed, to further refine our understanding of the history of the South American Monsoon during the last millennium. Characterization and interpretation of the second PC mode in particular will benefit from further sampling along the edges of the monsoon domain. Oceanic SST proxies along the coast of Brazil would be equally valuable in this regard. Decomposing the monsoon into its main modes of variability by means of Monte Carlo PCA will also facilitate the comparison between paleoclimatic proxies and earth system models (Benestad et al., 2017), slated to come online as part of the PMIP4/CMIP6 last millennium ensemble (Jungclaus et al., 2017).

Acknowledgments
We are grateful to ICMBio for permission to collect stalagmite samples. J. L. P. S. C. was supported by CNPq/Brazil with fellowship 140140207/2017-1. The research received financial support from FAPESP/Brazil (Grant PIRE FAPESP 2017/50085-3 to F. W. C. and fellowships 2016/15807-5 to V. F. N.; and INCLINE/USP to T. A. and F. W. C, and NSF OISE-1743738 to M. V. and 1103403 to R. L. E and H. C. M. D. acknowledges funding by the German Research Foundation (DFG) Grant DE 2398/3-1. The authors especially wish to thank Prof. Pedro Silva Dias for his valuable comments on this manuscript. The proxy time series used in this paper can be found in the references of Table 1.

References

Anchukaitis, K. J., & Tierney, J. E. (2013). Identifying coherent spatiotemporal modes in time-uncertain proxy paleoclimate records. *Climate Dynamics*, *41*(5-6), 1291–1306. https://doi.org/10.1007/s00382-012-1483-0

Apaéstegui, J., Cruz, F. W., Sifeddine, A., Vuille, M., Espinoza, J. C., Guyot, J. L., et al. (2014). Hydroclimate variability of the northwestern Amazon Basin near the Andean foothills of Peru related to the South American Monsoon System during the last 1600 years. *Climate of the Past*, *10*(6), 1967–1981. https://doi.org/10.5194/cp-10-1967-2014

Apaéstegui, J., Cruz, F. W., Vuille, M., Fohlmeister, J., Espinoza, J. C., Sifeddine, A., et al. (2018). Precipitation changes over the eastern Bolivian Andes inferred from speleothem (δ18O) records for the last 1400 years. *Earth and Planetary Science Letters*, *494*, 124–134. https://doi.org.10.1016/j.epsl.2018.04.048

Benestad, R., Sillmann, J., Thorarinsdottir, T. L., Guttorp, P., Mesquita, M. . S., Tye, M. R., et al. (2017). New vigour involving statisticians to overcome ensemble fatigue. *Nature Climate Change*, *7*(10), 697–703. https://doi.org/10.1038/nclimate3393

Bernal, J. P., Cruz, F. W., Stríkis, N. M., Wang, X., Deininger, M., Catunda, M. C. A., et al. (2016). High-resolution Holocene South American monsoon history recorded by a speleothem from Botuverá Cave, Brazil. *Earth and Planetary Science Letters*, *450*, 186–196. https://doi.org/10.1016/j.epsl.2016.06.008

Bird, B. W., Abbott, M. B., Vuille, M., Rodbell, D. T., Stansell, N. D., & Rosenmeier, M. F. (2011). A 2,300-year-long annually resolved record of the South American summer monsoon from the Peruvian Andes. *Proceedings of the National Academy of Sciences*, *108*(21), 8583–8588. https://doi.org/10.1073/pnas.1003719108

Carvalho, L. M., Jones, C., & Liebmann, B. (2004). The South Atlantic convergence zone: Intensity, form, persistence, and relationships with intraseasonal to interannual activity and extreme rainfall. *Journal of Climate*, *17*(1), 88–108. https://doi.org/10.1175/1520-0442(2004)017<0088:TSACZI>2.0.CO;2

Chaves, R. R., & Nobre, P. (2004). Interactions between sea surface temperature over the South Atlantic Ocean and the South Atlantic Convergence Zone. *Geophysical Research Letters*, *31*, L03204. https://doi.org/10.1029/2003GL018647

Chen, T. C., Weng, S. P., & Schubert, S. (1999). Maintenance of austral summertime upper-tropospheric circulation over tropical South America: The Bolivian high–Nordeste low system. *Journal of the Atmospheric Sciences*, *56*(13), 2081–2100. https://doi.org/10.1175/1520-0469(1999)056<2081:MOASUT>2.0.CO;2

Chiessi, C. M., Mulitza, S., Pätzold, J., Wefer, G., & Marengo, J. A. (2009). Possible impact of the Atlantic Multidecadal Oscillation on the South American summer monsoon. *Geophysical Research Letters*, *36*, L21707. https://doi.org/10.1029/2009GL039914

Cruz, F. W. Jr., Vuille, M., Burns, S. J., Wang, X., Cheng, H., Werner, M., et al. (2009). Orbitally driven east-west anti-phasing of South American precipitation. *Nature Geoscience*, *2*(3), 210–214. https://doi.org/10.1038/NGEO444

Deininger, M., McDermott, F., Mudelsee, M., Werner, M., Frank, N., & Mangini, A. (2017). Coherency of late Holocene European speleothem $\delta^{18}O$ records linked to North Atlantic Ocean circulation. *Climate Dynamics*, *49*((1-2), 595–618. https://doi.org/10.1007/s00382-016-3360-8

Deininger, M., Ward, B. M., Novello, V. F., & Cruz, F. W. (2019). Late Quaternary variations in the South American monsoon system as inferred by speleothems — New perspectives using the SISAL database. *Quaternary*, *2*(1), 6. https://doi.org/10.3390/quat2010006

Garreaud, R., Vuille, M., & Clement, A. C. (2003). The climate of the Altiplano: observed current conditions and mechanisms of past changes. *Palaeogeography, Palaeoclimatology, Palaeoecology*, *194*(1-3), 5–22. https://doi.org/10.1016/S0031-0182(03)00269-4

Garreaud, R. D., Vuille, M., Compagnucci, R., & Marengo, J. (2009). Present-day South American climate. *Palaeogeography, Palaeoclimatology, Palaeoecology*, *281*(3-4), 180–195. https://doi.org/10.1016/j.palaeo.2007.10.032

Haug, G. H., Hughen, K. A., Sigman, D. M., Peterson, L. C., & Röhl, U. (2001). Southward migration of the intertropical convergence zone through the Holocene. *Science*, *293*(5533), 1304–1308. https://doi.org/10.1126/science.1059725

Hoskins, B. J., & Ambrizzi, T. (1993). Rossby wave propagation on a realistic longitudinally varying flow. *Journal of the Atmospheric Sciences*, *50*(12), 1661–1671. https://doi.org/10.1175/1520-0469(1993)050<1661:RWPOAR>2.0.CO;2

Hurley, J. V., Vuille, M., & Hardy, D. R. (2016). Forward modeling of $\delta^{18}O$ in Andean ice cores. *Geophysical Research Letters*, *43*, 8178–8188. https://doi.org/10.1002/2016GL070150

Hurley, J. V., Vuille, M., Hardy, D. R., Burns, S. J., & Thompson, L. G. (2015). Cold air incursions, $\delta^{18}O$ variability, and monsoon dynamics associated with snow days at Quelccaya Ice Cap, Peru. *Journal of Geophysical Research: Atmospheres*, *120*, 7467–7487. https://doi.org/10.1002/2015JD023323

Intergovernmental Panel on Climate Change (IPCC) (Éd.) (2009). *Climate Change 2013 - The Physical Science Basis*. https://doi.org.10.1017/cbo9781107415324

Jones, C., & Carvalho, L. M. (2018). The influence of the Atlantic multidecadal oscillation on the eastern Andes low-level jet and precipitation in South America. *npj Climate and Atmospheric Science*, *1*(1), 40. https://doi.org/10.1038/s41612-018-0050-8

Jorgetti, T., da Silva Dias, P. L., & de Freitas, E. D. (2014). The relationship between South Atlantic SST and SACZ intensity and positioning. *Climate Dynamics*, *42*(11-12), 3077–3086. https://doi.org/10.1007/s00382-013-1998-z

Jungclaus, J. H., Bard, E., Baroni, M., Braconnot, P., Cao, J., Chini, L. P., et al. (2017). The PMIP4 contribution to CMIP6 – Part 3: The last millennium, scientific objective, and experimental design for the PMIP4 past1000 simulations. *Geoscientific Model Development*, *10*(11), 4005–4033. https://doi.org/10.5194/gmd-10-4005-2017

Kanner, L. C., Burns, S. J., Cheng, H., Edwards, R. L., & Vuille, M. (2013). High-resolution variability of the South American summer monsoon over the last seven millennia: insights from a speleothem record from the central Peruvian Andes. *Quaternary Science Reviews*, *75*, 1–10. https://doi.org/10.1016/j.quascirev.2013.05.008

Kodama, Y. (1992). Large-scale common features of subtropical precipitation zones (the Baiu frontal zone, the SPCZ, and the SACZ) Part I: Characteristics of subtropical frontal zones. *Journal of the Meteorological Society of Japan. Series II*, *70*(4), 813–836. https://doi.org/10.2151/jmsj1965.70.4_813

Laloyaux, P., de Boisseson, E., Balmaseda, M., Bidlot, J. R., Broennimann, S., Buizza, R., et al. (2018). CERA-20C: A coupled reanalysis of the Twentieth Century. *Journal of Advances in Modeling Earth Systems*, *10*, 1172–1195. https://doi.org/10.1029/2018MS001273

Lavielle, M. (2005). Using penalized contrasts for the change-point problem. *Signal Processing*, *85*(8), 1501–1510. https://doi.org/10.1016/j.sigpro.2005.01.012

Lenters, J. D., & Cook, K. H. (1999). Summertime precipitation variability over South America: Role of the large-scale circulation. *Monthly Weather Review*, *127*(3), 409–431. https://doi.org/10.1175/1520-0493(1999)127<0409:SPVOSA>2.0.CO;2

Ma, H. Y., Ji, X., Neelin, J. D., & Mechoso, C. R. (2011). Mechanisms for precipitation variability of the eastern Brazil/SACZ convective margin. *Journal of Climate*, *24*(13), 3445–3456. https://doi.org/10.1175/2011JCLI4070.1

Marengo, J. A., Liebmann, B., Grimm, A. M., Misra, V., Silva Dias, P. L., Cavalcanti, I. F. A., et al. (2012). Recent developments on the South American monsoon system. *International Journal of Climatology*, *32*(1), 1–21. https://doi.org/10.1002/joc.2254

Moquet, J. S., Cruz, F. W., Novello, V. F., Strikis, N. M., Deininger, M., & Karmann, et al. (2016). Calibration of speleothem $\delta^{18}O$ records against hydroclimate instrumental records in Central Brazil. *Global and Planetary Change*, *139*, 151–164. https://doi.org/10.1016/j.gloplacha.2016.02.001

Muza, M. N., Carvalho, L. M., Jones, C., & Liebmann, B. (2009). Intraseasonal and interannual variability of extreme dry and wet events over southeastern South America and the subtropical Atlantic during austral summer. *Journal of Climate*, *22*(7), 1682–1699. https://doi.org/10.1175/2008JCLI2257.1

Novello, V. F., Cruz, F. W., Karmann, I., Burns, S. J., Stríkis, N. M., Vuille, M., et al. (2012). Multidecadal climate variability in Brazil's Nordeste during the last 3000 years based on speleothem isotope records. *Geophysical Research Letters*, *39*, L23706. https://doi.org/10.1029/2012GL053936

Novello, V. F., Cruz, F. W., Moquet, J. S., Vuille, M., de Paula, M. S., Nunes, D., et al. (2018). Two millennia of South Atlantic Convergence Zone variability reconstructed from isotopic proxies. *Geophysical Research Letters*, *45*, 5045–5051. https://doi.org/10.1029/2017GL076838

Novello, V. F., Vuille, M., Cruz, F. W., Stríkis, N. M., de Paula, M. S., Edwards, R. L., et al. (2016). Centennial-scale solar forcing of the South American Monsoon System recorded in stalagmites. *Scientific Reports*, *6*(1), 24762. https://doi.org/10.1038/srep24762

Parsons, L. A., Yin, J., Overpeck, J. T., Stouffer, R. J., & Malyshev, S. (2014). Influence of the Atlantic Meridional Overturning Circulation on the monsoon rainfall and carbon balance of the American tropics. *Geophysical Research Letters*, *41*, 146–151. https://doi.org/10.1002/2013GL058454

Perez, L., García-Rodríguez, F., & Hanebuth, T. J. (2016). Variability in terrigenous sediment supply offshore of the Río de la Plata (Uruguay) recording the continental climatic history over the past 1200 years. *Climate of the Past*, *12*(3), 623–634. https://doi.org/10.5194/cp-12-623-2016

Salio, P., Nicolini, M., & Zipser, E. J. (2007). Mesoscale convective systems over southeastern South America and their relationship with the South American low-level jet. *Monthly Weather Review*, *135*(4), 1290–1309. https://doi.org/10.1175/MWR3305.1

Silva, V. B., & Berbery, E. H. (2006). Intense rainfall events affecting the La Plata Basin. *Journal of Hydrometeorology*, *7*(4), 769–787. https://doi.org/10.1175/JHM520.1

Sulca, J., Vuille, M., Silva, Y., & Takahashi, K. (2016). Teleconnections between the Peruvian central Andes and Northeast Brazil during extreme rainfall events in austral summer. *Journal of Hydrometeorology*, *17*(2), 499–515. https://doi.org/10.1175/JHM-D-15-0034.1

Thompson, L. G., Mosley-Thompson, E., Davis, M. E., Zagorodnov, V. S., Howat, I. M., Mikhalenko, V. N., & Lin, P. N. (2013). Annually resolved ice core records of tropical climate variability over the past~ 1800 years. *Science*, *340*(6135), 945–950. https://doi.org/10.1126/science.1234210

Utida, G., Cruz, F. W., Etourneau, J., Bouloubassi, I., Schefuß, E., Vuille, M., et al. (2019). Tropical South Atlantic influence on Northeastern Brazil precipitation and ITCZ displacement during the past 2,300 years. *Scientific Reports*, *9*(1), 1698. https://doi.org/10.1038/s41598-018-38003-6

Vuille, M., Burns, S. J., Taylor, B. L., Cruz, F. W., Bird, B. W., Abbott, M. B., et al. (2012). A review of the South American monsoon history as recorded in stable isotopic proxies over the past two millennia. *Climate of the Past*, *8*(4), 1309–1321. https://doi.org/10.5194/cp-8-1309-2012

Vuille, M., & Werner, M. (2005). Stable isotopes in precipitation recording South American summer monsoon and ENSO variability: observations and model results. *Climate Dynamics*, *25*(4), 401–413. https://doi.org/10.1007/s00382-005-0049-9

Wang, X., Edwards, R. L., Auler, A. S., Cheng, H., Kong, X., Wang, Y., et al. (2017). Hydroclimate changes across the Amazon lowlands over the past 45,000 years. *Nature*, *541*(7636), 204–207. https://doi.org/10.1038/nature20787

Wortham, B. E., Wong, C. I., Silva, L. C. R., McGee, D., Montañez, I. P., Troy Rasbury, E., et al. (2017). Assessing response of local moisture conditions in central Brazil to variability in regional monsoon intensity using speleothem 87 Sr/86 Sr values. *Earth and Planetary Science Letters*, *463*, 310–322. https://doi.org/10.1016/j.epsl.2017.01.034

Zhou, J., & Lau, K. (1998). Does a Monsoon Climate Exist over South America? *Journal of Climate*, *11*, 1020–1040. https://doi.org/10.1175/1520-0442(1998)011<1020:DAMCEO>2.0.CO;2

References From the Supporting Information

da Silva, A. E., & de Carvalho, L. M. V. (2007). Largescale index for South America Monsoon (LISAM). *Atmospheric Science Letters*, *8*(2), 51–57. https://doi.org/10.1002/asl.150

North, G. R., Bell, T. L., Cahalan, R. F., & Moeng, F. J. (1982). Sampling errors in the estimation of empirical orthogonal functions. *Monthly Weather Review*, *110*(7), 699–706. https://doi.org/10.1175/1520-0493(1982)110<0699:SEITEO>2.0.CO;2